*J. Indian Inst. Sci.*, May–Aug. 2003, **83**, 61–71


# Two-wave mixing and light-induced absorption dynamics in photorefractive $BaTiO_3$ crystals

RAVINDER KUMAR BANYAL AND B. RAGHAVENDRA PRASAD*
Indian Institute of Astrophysics, Bangalore 560 034, India.
email: brp@iiap.res.in; Phone: 91-80-25530672; Fax: 91-80-25534043.

**Abstract**

Steady-state and temporal measurements of TWM and LIA have been carried out in PR $BaTiO_3$ crystals at different wavelengths and intensities of laser light. The observed behavior is interpreted in terms of two-center charge transport model for PR materials. The rate equations were solved to derive an analytical expression for steady-state absorption changes. Various model parameters like build-up and decay rates, thermal excitation rates, and two-wave coupling gain have been obtained and compared with the earlier studies.

**Keywords**: Two-wave mixing, photorefractive, light-induced absorption.

## 1. Introduction

Photorefractive (PR) materials show light-induced refractive index changes that can be exploited in a variety of applications [1] like holographic data storage, information processing, coherent image amplification, nonlinear filtering, phase conjugation and optical switching, etc. One such material is $BaTiO_3$ that has attractive PR properties like high values of electro-optic coefficient, fast response time and excellent phase conjugate reflectivity. Large electro-optic coefficient allows one to achieve very high gain coefficient in two-beam coupling. Applications like real-time holography or optical phase conjugation used in distortion correction in a time-varying distortive media require a very fast PR response of the crystal. Response time depends on the input beam intensity; however, beam fanning and light-induced absorption (LIA) can deplete pump as well as signal beam intensities. Therefore, it is vital to study these limiting factors that can restrain the PR performance of the crystal in various applications.

The presence of impurity atoms like Fe, Mn, Cu and Co (also called primary or deep centers) is thought to be responsible for the PR effect. A model based on single carrier primary centers [2] satisfactorily explains the PR effect in most of the cases. However, it fails to explain the sublinear dependence of the two-beam coupling coefficients and typical nonlinear dependence of photoconductivity and absorption coefficients at higher intensities in $BaTiO_3$ crystals. Increase in absorption due to illumination of $BaTiO_3$ was first discovered in 1987 by Motes and Kim [3]. In 1988, Brost *et al*. [4] explained this effect by a two-center charge transport model. A two-center model postulates the existence of secondary PR centers (also called shallow traps) that can account for most of these intensity-dependent effects. This model was further confirmed by several experiments [5]–[10] carried out using two-wave mixing (TWM) and LIA in $BaTiO_3$. Therefore, it is important to investigate and understand the characteristics of these impurities both for theory and applications. To identify the impurity defects that are responsible for the PR effect is not straightforward. However, different methods like measurement of photoconductivity, temperature and LIA studies, electron spin resonance (ESR) spectrum, and linear absorption spectrum can reveal the information of shallow traps. In this paper, we present the experimental

* Author for correspondence.

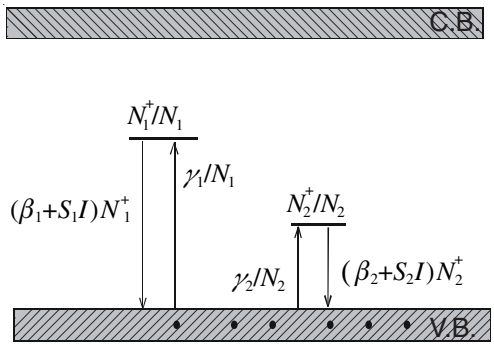


FIG. 1. Energy-level diagram for two-center model in $p$-type $BaTiO_3$ crystal.

results of temporal and steady-state behavior of TWM and LIA in a pure and rhodium (Rh)-doped $BaTiO_3$ crystal. We also report an anomalous LIA in Rh-doped $BaTiO_3$ sample that has not been reported in earlier studies.

## 2. Light-induced absorption

LIA is characterized by increase in absorption coefficient with laser intensity. It can be induced by uniformly illuminating the crystal with strong pump beam at one wavelength and observed by monitoring the transmission of a weak probe beam through the crystal at different wavelength. It has already been shown that intensity-dependent absorption is consistent with two-center charge transport model [4]. It is based on the assumption that two different impurity centers, each of them occurring in different valence states, are present. The first is deep and the second is shallow with respect to the valence band edge. Figure 1 shows two-center energy level diagram for $p$-type crystal, where holes are the dominant charge carriers. $N_1(N_1^+$ and $N_2\,(N_2^+)$ are the densities of the empty (filled) deep and shallow impurities, respectively, whereas $N_{1T}= N_1+ N_1^+$ and $N_{2T}= N_2 + (N_2^+)$ are the total deep and shallow center densities. The rate equations governing the charge transport for the deep and shallow levels are [4]:

$$\frac{dN_i^+}{dt} = -(S_iI + \beta_i)\,N_i^+ + \gamma_i\,(N_{iT} - N_i^+)n_h, \tag{1}$$

$i=1,2$

where $S$ is photon-absorption cross-section, $\gamma$, the recombination coefficient, $\beta$, the thermal ionization rate, $I$, the laser intensity and $n_h$, the free carrier (hole) density. Subscript $i=1, 2$ refers to deep and shallow levels, respectively. Illuminating the crystal with laser light causes photo-ionization and redistribution of the charges between deep and shallow traps. This results in LIA change

$$\Delta\alpha = \sum_{i=1,2} S_i\,[N_i^+ - N_i^+(0)], \tag{2}$$

where $N_i^+(0)$ is dark concentration of filled traps. The charge conservation requires

$$\sum_{i=1,2} N_i^+ + n_h = N_c, \tag{3}$$

where $N_c$ is the density of compensating charge centers that do not participate in PR effect, but required to maintain overall charge neutrality of the crystal. We can neglect the hole concentration in eqn (3) as it remains small compared to the impurity concentration [5]. In the *steady-state* condition, $dN_i^+/dt = 0$, so we solved eqns (1)–(3), to get

$$\Delta\alpha = \sum_{i=1,2} S_i [N_i (1 - \frac{S_i I + \beta_i}{\gamma_i A}) N_i^+(0)], \tag{4}$$

where

$$A = \frac{N_1 \gamma_2 (S_1 I + \beta_1) + N_2 \gamma_1 (S_2 I + \beta_2)}{N_1 + N_2 - N_c) \gamma_1 \gamma_2}. \tag{5}$$

Time evolution of the LIA absorption in the build-up process [6] can be described by

$$\Delta\alpha(t) = [1 - \exp(t/\tau)], \tag{6}$$

$$\tau^{-1} = S_2 I + \beta_2 + \gamma_2 n_h. \tag{7}$$

Because of the approximate proportionality between $n_h$ and $I$, eqn (7) can be rewritten as

$$\tau^{-1} = a I + \beta_2, \tag{8}$$

where $\alpha$ is a factor that is independent of intensity. Equation (8) can be used to determine the thermal excitation rate $\beta_2$.

### 3. Two-wave mixing

A nonuniform illumination of crystal by coherent light (such as two-beam interference pattern) can photoexcite the charges from impurity sites to the conduction band. Under the influence of diffusion or drift (in the presence of external field), charges are migrated from brighter region and subsequently trapped in darker region. Such redistribution of charges between brighter and darker region leads to the development of internal electric field $E_{sc}$ which in turn modulates the refractive index of the material via electro-optic effect, i.e.

$$\Delta n = \frac{-r_{\text{eff}}\, n^3}{2} E_{sc}, \tag{9}$$

where $r_{\text{eff}}$ is the effective electro-optic coefficient and $n$, the refractive index of the crystal. A $\pi/2$ phase shift between refractive index grating and illuminating interference pattern leads to energy transfer from one beam to another. This happens because the phase grating diffracts each beam in the direction of the other with additional phase shift of $\pm\,\pi/2$. In one case, diffracted beam interferes destructively ($\pi/2 + \pi/2 = \pi$) with transmitted beam thereby diminishing the intensity; on the other hand, a constructive interference ($\pi/2 + \pi/2 = \pi$) between diffracted and transmitted beam leads to increase in energy for the second case. For the appropriate orientation of the crystal, the signal beam $I_s$ experiences a gain at the cost of pump beam $I_p$. Transmission of the signal beam, after traversing the crystal length $L$ is given [1] by,

$$\frac{I_s(L)}{I_s(0)} = \frac{[I_s(0) + I_p(0)] \exp[(\Gamma - \alpha) L]}{I_p(0) + I_s(0) \exp(\Gamma L)}. \tag{10}$$

The beam coupling gain $\Gamma$ is defined as

$$\Gamma = 4\pi^2 \frac{n^3 k_B T}{q\lambda} \frac{\Lambda_d}{\Lambda_d^2 + \Lambda_o^2} r_{\text{eff}}, \tag{11}$$

where $\Lambda_d$, $k_B$, $T$, $q$, $\lambda$ are grating period, Boltzmann constant, temperature, electronic charge and light wavelength, respectively, and

$$\Lambda_o = \frac{2\pi}{q} \left( \varepsilon \varepsilon_o \frac{k_B T}{N_E} \right)^{1/2} \tag{12}$$

is Debye screening length, $N_E = NN^+/(N + N^+)$ is effective trap density and $\varepsilon$, dielectric constant. Experimentally, the photorefractive gain, $\gamma_o$, as measured in laboratory, is given by,

$$\gamma_o = \frac{I_s(L) \text{ with pump on}}{I_s(L) \text{ with pump off}}. \tag{13}$$

Therefore, the measurement of $\gamma_o$ along with eqn (10) provides a direct means of determining $\Gamma$. The effective trap density $N_E$ can be estimated using eqn (12), by noting that beam coupling gain $\Gamma$ in eqn (11) is maximum when $\Lambda_o = \Lambda_d = \lambda \sin\theta$. The time constants involved in the grating build-up and decay are also an important parameter in evaluating the figure of merit of photorefractive crystals. Kukhtarev *et al*. [2] have given a complete analysis of the dynamics of grating formation and erasure for continuous wave illumination. Time required to write a refractive index grating depends on the efficiency of charge generation and transport mechanism. A simple expression for the time dependence of space charge field during the grating recording is given by,

$$\Delta E_{sc} = m E_{sc} [1 - \exp(-t/\tau_{\text{eff}})]. \tag{14}$$

Similarly, a grating erasure can be accomplished by uniform illumination of the crystal. The decay of space charge field during the erasure process can be written as,

$$\Delta E_{sc} = I E_{sc}^{o} \exp(-t/\tau_{\text{eff}})], \tag{15}$$

where $E_{sc}$ is the initial amplitude and $E_{sc}^{o}$, the maximum amplitude of the space charge field obtained in steady state, $I$, the irradiance of the erasing beam, $m$, the intensity modulation index, and $\tau_{\text{eff}}$, the effective time constant for the crystal response. As in the case of LIA, the $\tau_{\text{eff}}$ can have multiple components due to the presence of different impurity traps in the crystal. In general, the value of $\tau_{\text{eff}}$ may be a function of different parameters like pump and signal beam intensity, light wavelength, modulation index, $m$, and dark conductivity, etc.

## 4. Experiments and results

We used $0^o$ cut as-grown undoped and Rh-doped $BaTiO_3$ crystals with dimensions ($c \times a \times a$), $6.72 \times 6.28 \times 5.5$ mm and $6.6 \times 5.8 \times 4.2$ mm, respectively. Figure 2 shows the schematic for the experimental set-up. An expanded pump beam $I_p$ at wavelength $\lambda_p$ illuminates the crystal, whereas a weak signal beam $I_s$ at different wavelength $\lambda_s$ acts as a probe to study the change in absorption. Different pump and probe wavelengths were chosen in order to eliminate the possibility of beam coupling effects that can rise if both the beams are coherent (Table I).

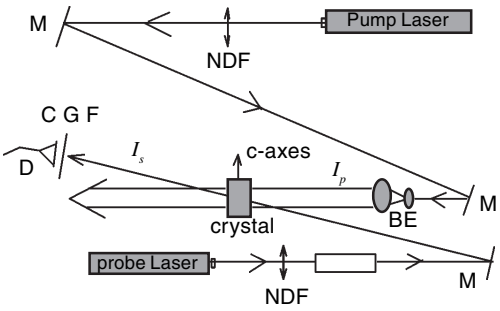


FIG. 2. Schematic of the experimental set-up. M: mirrors; NDF: neutral density filter; GP: Glan laser polarizer; D: detector; BE: beam expander; CGF: colour glass filter; $I_p$: pump beam; and $I_s$: probe beam.

The small beam-crossing angle ensures a complete and uniform overlap of the beams inside the crystal. The diameter of the probe beam inside the crystal was approximately 2 mm. The intensity of the pump beam was varied from ~3 $\mu$ Wcm$^{-2}$ to 16 Wcm$^{-2}$ using compensated neutral density filter (Model: 925B; Newport). Pump beam illumination was controlled using electromechanical shutter. The transmission of the probe was monitored using computer-controlled optical power meter (Model: 4832-C Multichannel Optical Power Meter; Newport). Both the beams were made o-polarized to minimize the beam fanning and scattering effects which otherwise could be mistaken for absorption. Appropriate color glass filters along with a small pin hole were used to prevent the pump beam entering the detector. Figure 3 (a) shows the transmission of the probe through undoped $BaTiO_3$ crystal as a function of time. For $t < t_0$ when pump beam is off, the probe beam power remains constant at 1 $\mu$ W. Once the pump beam was switched on at $t = t_0$, the transmission of the probe beam begins to fall and reaches a steady-state value due to LIA. It starts rising again after the pump is turned off at $t = t_1$. Photo-induced change in absorption coefficient $\Delta\alpha$ can be determined using the relation

$$\frac{I_s \text{ (with } I_p \text{ on)}}{I_s \text{ (with } I_p \text{ off)}} = \exp(-\Delta\alpha L) \tag{16}$$

where $L$ is the effective length of the crystal and $I_s$ and $I_p$, the probe and pump beam intensities, respectively. The temporal evolution of light-induced absorption change calculated using eqn (16) is shown in Fig. 3(b). A wavelength-specific anomalous temporal evolution of absorption was observed in Rh-doped $BaTiO_3$ (Fig. 4). After the pump beam was turned on at $t = t_0$, an unexpected fall in absorption could be noticed for some time, which is then followed by usual absorption rise. Contrary to the behavior shown in Fig. 3 (b), a further absorption increase was

**Table I**
**Light wavelengths and sources used in LIA measurements**

| | Wavelength (nm) | Source | Model |
|---|---|---|---|
| Probe ($\lambda_s$) | 633 | He-Ne | 05-LHR-151; Melles Griot |
| | 543 | He-Ne | 1208-2; JDS Uniphase |
| | 750 | Ti:sapphire | 3900S; Spectra Physics |
| | 800 | Ti:sapphire | |
| Pump ($\lambda_p$) | 488 | Argon-ion | BeamLok™ 2085; Spectra Physics |
| | 514 | Argon-ion | |

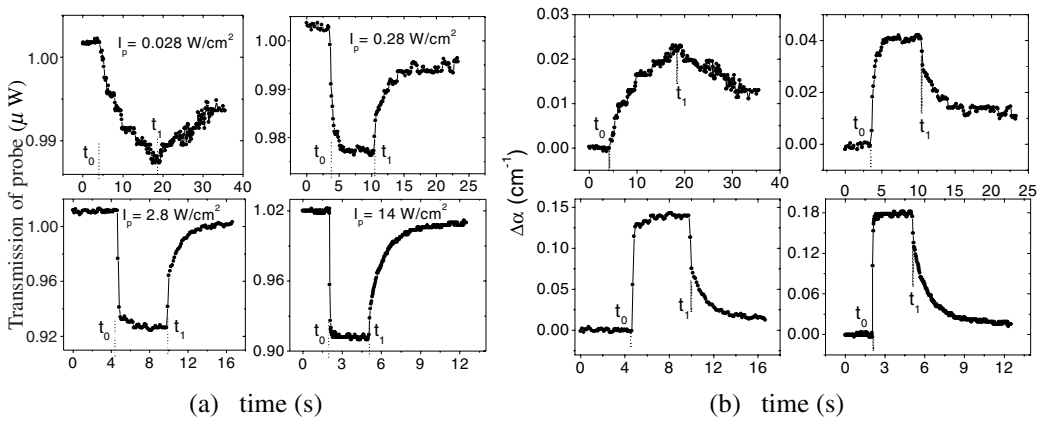


FIG. 3. Probe beam transmission ($\lambda_s$= 633 nm) through undoped $BaTiO_3$ crystal when illuminated by pump at 514 nm at different intensities (a), and corresponding LIA change (b).

observed even after the pump beam was put off at $t = t_1$. For clarity, we denote the magnitude of this additional absorption change by $\delta$ and $\delta'$ in Fig. 4.

Dependence of $\delta$ and $\delta'$ on pump intensity is plotted in Fig. 5. We notice a linear change in $\delta$ up to ~ 0.23 $\mu$ Wcm$^{-2}$, beyond which it is almost constant and falls at higher intensities. Physical mechanism responsible for this particular behavior is not very clear. Temperature-dependent absorption studies [10],[11] in the past have shown that rise in temperature can cause decrease in absorption and vice versa.

In our opinion, new wavelength-specific photorefractive centers are either created or become active due to light-induced thermal effects that modify the absorption dynamics in an unusual manner. However, we must add that there is no strong evidence against the possibility of additional crystal defects which could possibly lead to similar results.

Absorption build-up curves for both the crystals (e.g. region between $t_0$ and $t_1$ in Fig. 3 (b)) follow mono-exponential rise as described by eqn (6). Rise time constant $\tau$ was calculated by fitting the experimental data into eqn (6). Figure 6 shows the plot of absorption rise time vs intensity of the pump beam. We note that response time decreases with intensity. We fitted the intensity power coefficients $x$ according to the relation $\tau \propto I^{-x}$ and found that absorption rise has sublinear intensity dependence. The value of $x$ was found to vary between ~0.4–1.0 for

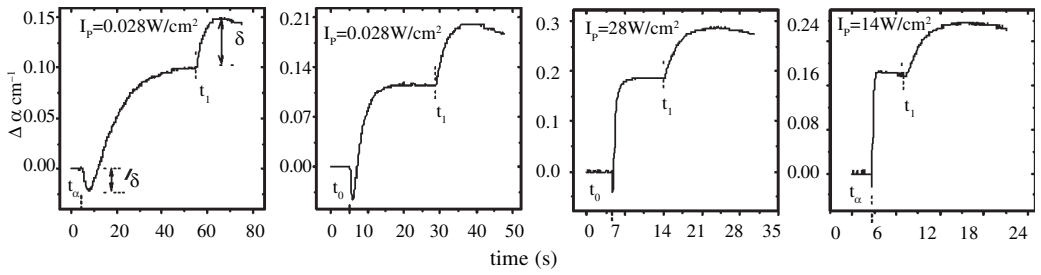


FIG. 4. Temporal evolution of anomalous absorption in $BaTiO_3$ at 633 nm probe and 514 nm pump beam at different intensities.

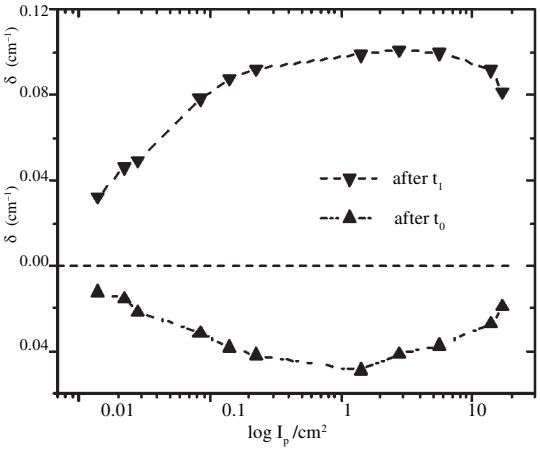


FIG. 5. Variation of anomalous absorption with pump beam intensity.

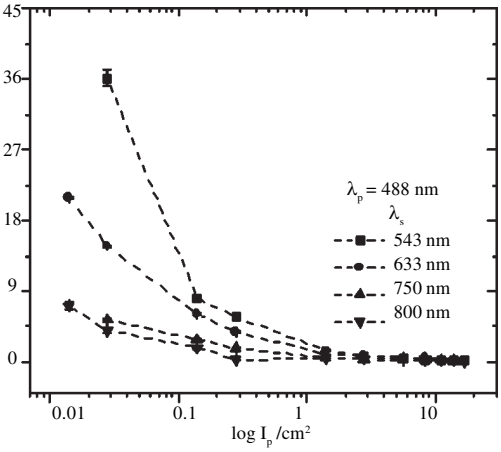


FIG. 6. Absorption rise time constant $\tau$ vs pump beam intensity.

Rh-doped and ~0.6–2.0 for undoped $BaTiO_3$ crystal. Therefore, the observed sublinear dependence of photorefractive grating formation and decay time scales in two-wave mixing [12] can be attributed to the sublinear response of intensity-dependent absorption, because the steady state in photorefractive grating (formation and decay) cannot be reached until LIA reaches the steady state.

Measurements of the steady-state LIA changes at different pump and probe wavelengths have also been carried out. The steady-state absorption change $\Delta\alpha$ for the two crystals at different probe wavelengths as a function of $I_p$ is shown in Fig. 7. Experimental data are represented by symbols, whereas the solid lines are theoretical curves calculated using eqn (4). Crystal parameters that best fit our data are given in Table II for $\lambda_p = 488$ nm (514 nm). The thermal excitation rates $\beta_2$ calculated using eqn (8), at different pump and probe wavelengths were found to be 0.1–0.3 and 0.5–0.6 $s^{-1}$ for Rh-doped and undoped $BaTiO_3$ crystals, respectively. These values are considerably smaller than the results reported in Brost *et al*. [4] and Buse and Bierwirth [5]. However, recent studies on three-level (one deep and two shallow) charge transport model [13] show that one of the shallow levels has similar thermal excitation rate that we found in our measurements. We also note that pump beam at 488 nm induces more absorption than at 514 nm for both the crystals because $S$ (488 nm) ≥ $S$ (514). In Rh-doped $BaTiO_3$, $\Delta\alpha$ was found to increase with increases in probe wavelengths, whereas the opposite is true for undoped sample. This indicates that the origin of secondary centers is different in both the crystals. The fact is that thermal ionization rate $\beta_2$ for undoped crystal is relatively higher than for Rh-doped $BaTiO_3$ and the pump beam intensity at which the absorption saturates is higher for undoped $BaTiO_3$ than for Rh-doped crystal.

The dark decay of LIA is associated with the loss of shallow and deep trap population by thermal ionization. In general, the dark decay process of LIA can be described by a double exponential function as,

$$\Delta\alpha(t) = a_0 + a_1 \exp(-t/\tau_1) + a_2 \exp(t/\tau_2), \tag{17}$$

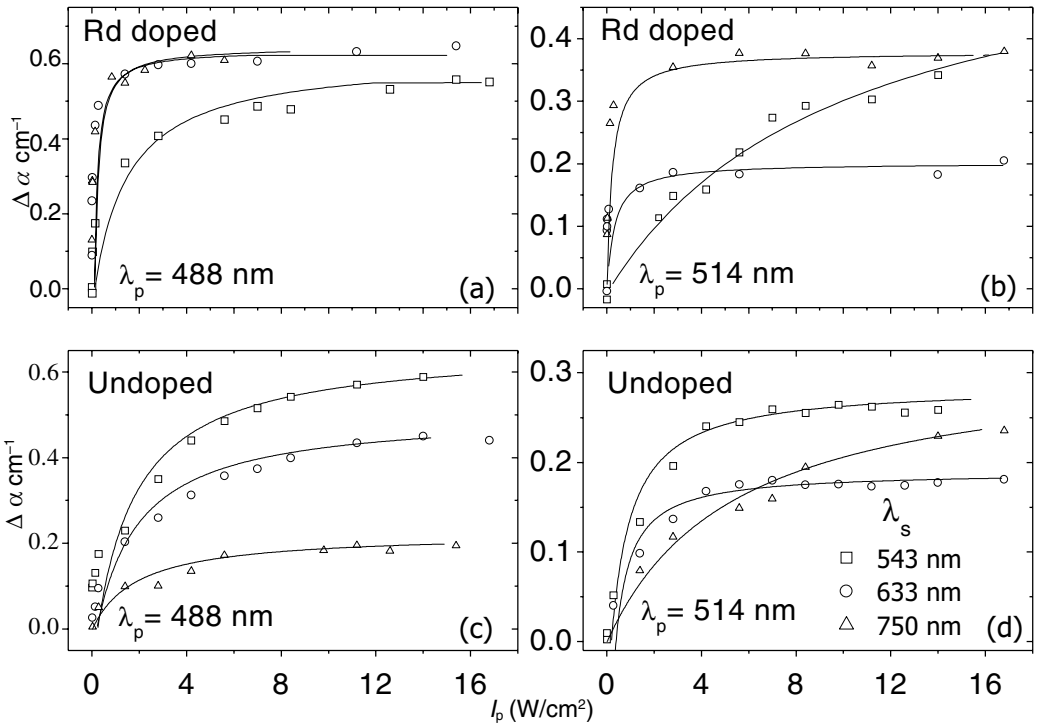


FIG.7. Steady-state light-induced absorption change $\Delta\alpha$ vs. pump beam intensity at different probe wavelengths. (a)–(b) for Rh-doped and (c)–(d) for undoped $BaTiO_3$ crystal.

where $\tau_1$ and $\tau_2$ are the fast and slow decay time constants, respectively. A typical dark decay of $\Delta\alpha$ (normalized to its maximum value) after blocking the pump beam at $t = 0$ is shown in Fig. 8. From the dark decay measurements of LIA in Rh-doped $BaTiO_3$ we note that the dark decay at 543 nm probe and 488 nm pump occurs in two separate steps. It showed an initial fast relaxation having two time constants, $\tau_1 \sim 50$ ms and $\tau_2 \sim 0.7$ s, followed by a slow relaxation with longertime constant of ~60 s. At 633 nm probe wavelength, a slow mono-exponential decay with $\tau_2 \sim 62$ s

**Table II**

**Crystal parameters used for theoretical calculations**

| Undoped $BaTiO_3$ | | | | Rh: $BaTiO_3$ | | | |
|---|---|---|---|---|---|---|---|
| $N_{1T} = 7.0 \times 10^{16}$ cm$^{-3}$; $N_1^+(0) = 6.9 \times 10^{16}$ cm$^{-3}$; $N_{2T} = 4.0 \times 10^{16}$ cm$^{-3}$; $N_2^+(0) = 8.0 \times 10^{11}$ cm$^{-3}$; $n_h(0) = 1.0 \times 10^6$ cm$^{-3}$; $\gamma_1 = 3.0 \times 10^{-8}$ cm$^3$ s$^{-1}$; $\gamma_2 = 1.0 \times 10^{-8}$ cm$^3$ s$^{-1}$; $\beta_1 = 8.0 \times 10^{-3}$ s$^{-1}$ | | | | $N_{1T} = 2.6 \times 10^{18}$ cm$^{-3}$; $N_1^+(0) = 2.57 \times 10^{18}$ cm$^{-3}$; $N_{2T} = 8.0 \times 10^{17}$ cm$^{-3}$; $N_2^+(0) = 3.8 \times 10^{14}$ cm$^{-3}$; $n_h(0) = 8.0 \times 10^5$ cm$^{-3}$; $\gamma_1 = 5.0 \times 10^{-8}$ cm$^3$ s$^{-1}$; $\gamma_2 = 2.8 \times 10^{-8}$ cm$^3$ s$^{-1}$; $\beta_1 = 1.5 \times 10^{-4}$ s$^{-1}$ | | | |
| $\lambda_s$ (nm) | $S_1 \times 10^{-17}$ (cm$^2$) | $S_2 \times 10^{-16}$ (cm$^2$) | $\beta_2$ (s$^{-1}$) | $\lambda_s$ (nm) | $S_1 \times 10^{-17}$ (cm$^2$) | $S_2 \times 10^{-16}$ (cm$^2$) | $\beta_2$ (s$^{-1}$) |
| 543 | 7.0 (2.2) | 1.6 (1.0) | 10 (5) | 543 | 5.2 (6.0) | 7.0 (4.2) | 1.0 (3.2) |
| 633 | 7.4 (2.2) | 1.3 (3.0) | 10 (5) | 633 | 7.4 (2.2) | 8.0 (1.4) | 0.2 (0.04) |
| 750 | 1.7 (2.8) | 1.0 (2.8) | 10 (5) | 750 | 1.7 (2.8) | 3.3 (6.5) | 0.1 (0.1) |

Note: $\lambda_p = 488$ nm (514 nm)

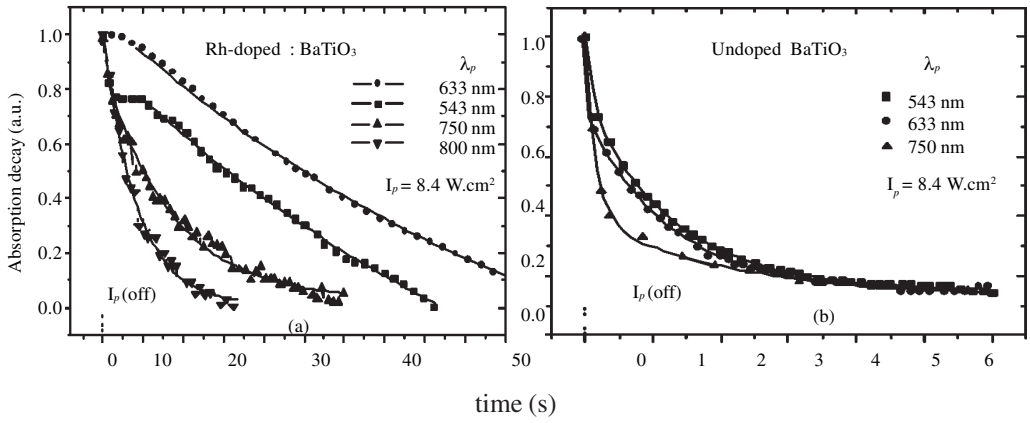


FIG. 8. Typical dark decay process of LIA change observed at 488 nm pump and different probe wavelengths (a) for Rh-doped: $BaTiO_3$ and (b) for undoped $BaTiO_3$. The symbols refer to measured result and solid curves are exponential fit to the experimental data.

alone was observed. Decay at wavelengths 750 nm and 800 nm was again found to be mono-exponential with $\tau_2 \sim 7.25(6.25)$ s, and $\tau_2 \sim 5.82(5.42)$ s, respectively at 488 nm (514 nm) pump. This indicates that at longer wavelength (≥ 633 nm) only one shallow level contributes to the LIA. The values reported by Brost and Motes [14], and Kaczmarek *et al*. [15] for ~6–10 s, and Corner *et al*. [16] for ~7 s are in close agreement with our measurements. This origin of the decay is attributed to $Rh^{4+/5+}$ levels [17]. For undoped $BaTiO_3$ crystal, we observed double exponential decay at 543 and 633 nm probe wavelengths, whereas the decay at 750 and 800 nm was mono-exponential (Table III). The reported values of two-decay constants by Song *et al.* [13] closely match our results. It should be pointed out that the observations of different time constants need not necessarily be identified with different shallow traps as the local heating of the crystal at different pump wavelengths can give rise to different thermal excitation rate for the same shallow level.

A standard set-up (shown in the inset of Fig. 9) was used to study the two-wave mixing in both the crystals. The direction of the c-axes of the crystal is chosen so that the energy is transferred from the pump beam to the signal beam. To write a refractive index grating, the path difference between the two interacting beams is kept well within the coherent length of the laser. The external beam-crossing angle was fixed at 35° and photorefractive gain $\gamma_o$ was measured at different intensity ratios $m = I_p/I_s$ by varying $I_s$ at fixed pump power. Figure 10 (a) shows the plot of $\gamma_o$ as a function of $m$. The gain was also measured at different beam crossing angles (Fig. 10 (b)) at fixed $m$. The optimum beam-crossing angles that corresponds to maximum gain for Rh-doped and undoped $BaTiO_3$ crystals are found to be ~ 30° and 40°, respectively. The grating decay was monitored by putting the signal beam off at $t_1$ (Fig. 9). Further analysis of the data revealed that rise and decay of grating have bi-exponential form with two time constants. Again the origin of different time constants can be attributed to the presence of deep and shallow impunity centers. Grating build-up and decay time scales observed in two-wave mixing are not very different from that found in absorption build-up and decay processes. Therefore, it will not be inappropriate to assert that absorption dynamics governs the TWM dynamics of the crystal to a great extent.

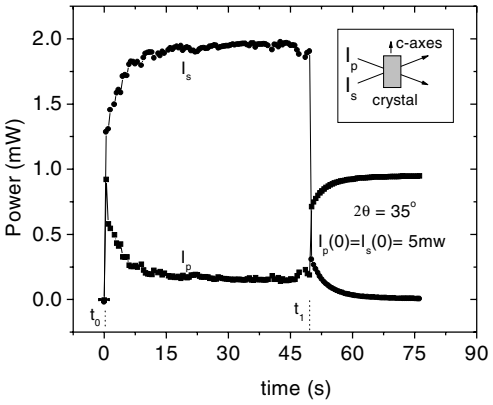


FIG. 9. Two-wave energy coupling in Rh-doped $BaTiO_3$ crystal at 488 nm.

**Table III**
**Decay time constants for undoped $BaTiO_3$ at 488 nm (514 nm) pump**

| $\lambda_s$(nm) | $\tau_1$(s) | $\tau_2$(s) |
|---|---|---|
| 543 | 0.10(0.12) | 1.25(1.30) |
| 633 | 0.13(0.12) | 1.50(1.40) |
| 750 | 0.57(0.53) | ….. |

## 5. Conclusion

We have presented a detailed experimental studies on the light-induced absorption and two-wave mixing in undoped and Rh-doped $BaTiO_3$ crystals. Various parameters pertaining to the temporal and steady-state behavior of LIA have been obtained and compared with the earlier results. We also observed an unusual absorption dynamics at specific pump (514 nm) and probe (633 nm) combination. In our opinion, the result of light-induced thermal effects is to create (new) or activate (already existing) impurity traps that are highly wavelength specific in terms of their energy levels and absorption cross-section. This needs to be probed separately by performing temperature-dependent absorption studies in future. In conclusion, we wish to emphasize that the light-induced absorption can greatly influence the dynamics of two-wave mixing and holographic grating recording in photorefractive crystals. Therefore, the effect of LIA needs to be properly understood and incorporated in any device application based on photorefractive crystals.

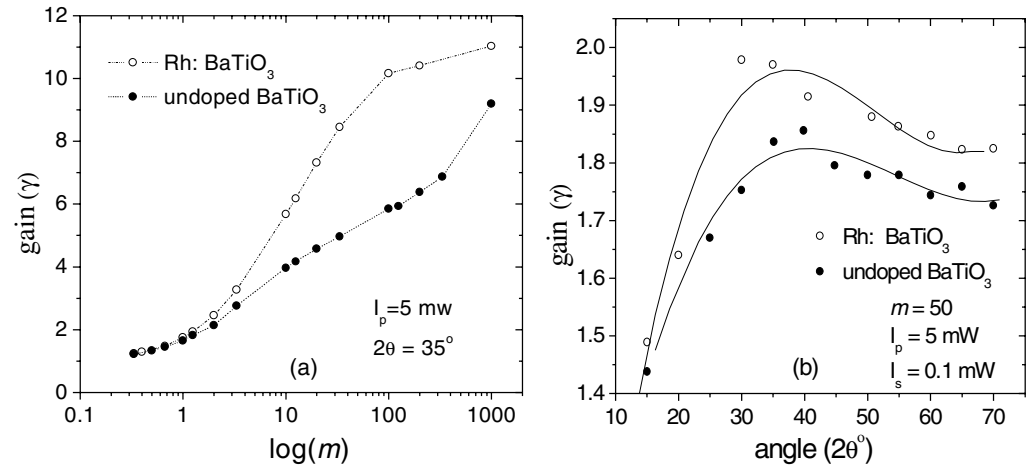


FIG.10. (a) Plot of gain vs intensity ratio *m* (b) gain vs beam-crossing angle measured at 488 nm.

## Acknowledgements

This work was carried out at CREST (Center for Research and Education in Science and Technology) campus of the Indian Institute of Astrophysics, Bangalore.

## References

1. P. Günter and J.-P. Huignard (eds), *Photorefractive materials and their applications*, I and II, Vols 61 and 62 of Topics in Applied Physics, Springer-Verlag, 1988.

2. N. V. Kukhtarev, V. B. Markov, S. G. Odulov, M. S. Soskin and V. L. Vinetskii, Holographic storage in electrooptic crystals. I. Steady-state, *Ferroelectrics*, **22**, 949–960 (1979).

3. A. Motes and J. J. Kim, Intensity-dependent absorption coefficients in photorefractive $BaTiO_3$ crystal, *J. Opt. Soc. Am. B*, **4**, 1379–1387 (1987).

4. G. A. Brost, R. A. Motes and J. R. Rotgé, Intensity-dependent absorption and photorefractive effects in barium titanate, *J. Opt. Soc. Am. B*, **5**, 1879–1885 (1988).

5. K. Buse and T. Bierwirth, Dynamics of light-induced absorption in $BaTiO_3$ and application for intensity stabilization, *J. Opt. Soc. Am. B*, **12**, 629–638 (1995).

6. L. Holtmann, M. Unland, E. Krätzig and G. Godefroy, Conductivity and light-induced absorption in $BaTiO_3$, *Appl. Phys. A*, **51**, 13–17 (1990).

7. P. Tayebati and D. Mahgerefteh, Theory of photorefractive effect for $Bi_{12}$ $SiO_{22}$ and $BaTiO_3$ with shallow traps, *J. Opt. Soc. Am. B*, **8**, 1053–1064 (1991).

8. J. Y. Chang, C. R. Chinjen, S. H. Daun, C. Y. Haung, R. H. Tsou, J. N. Cheng and C. C. Sun, The optical and photorefractive properties of reduced Rh-doped $BaTiO_3$ at wavelength of 514 nm, *Opt. Commun.*, **153**, 106 –110 (1998).

9. A. Brignon, D. Geffroy, J.-P. Huignard, M. H. Garrett and I. Mnushkina, Experimental investigation of the photorefractive properties of rhodium-doped $BaTiO_3$ at 1.06 μm, *Opt. Commun.*, **137**, 311–316 (1997).

10. A. Motes, G. Brost J. Rotgé and J.J. Kim Temporal behavior of the intensity-dependent absorption in photorefractive $BaTiO_3$, *Opt. Lett.*, **13**, 509–511 (1988).

11. Y. Li, D. Trung, B. Zhang, Y. Segawa and T. Itoh, Temperature dependence of light-induced absorption in reduced Co:KNSBN crystal with multiple shallow traps, *Proc. SPIE*, **3554**, 33–39 (1998).

12. D. Mahgerefteh and J. Feinberg, Explanation of the apparent sublinear photoconductivity of photofractive barium titanate, *Phys. Rev. Lett.*, **64**, 2195–2198 (1990).

13. H. Song, S. X. Dou, M. Chi, H. Gao, Y. Zhu and P. Ye, Studies of shallow levels in undoped and rhodium-doped barium titanate, *J. Opt. Soc. Am. B*, **15**, 1329–1334 (1998).

14. G. A. Brost and R. A. Motes, Photo-induced absorption in photorefractive barium titanate, *Opt. Lett.*, **15**, 538–540 (1990).

15. M. Kaczmarek, G. W. Ross, R. W. Eason, M. J. Damzen, R. Ramos-Garcia and M. H. Garrett, Intensity-dependent absorption and its modeling in infrared sensitive rhodium-doped $BaTiO_3$, *Opt. Commun.*, **126**, 175–184 (1996).

16. L. Corner, R. Ramos-Garcia, A. Petris and M. J. Damzen, Experimental and theoretical characterization of rhodium-doped barium titanate, *Opt. Commun.*, **143**, 165–172 (1997).

17. H. Krose, R. Scharfschwerdt, O. F. Schirmer and H. Hesse, Light-induced charge transport in $BaTiO_3$ via three charge states of rhodium, *Appl. Phys. B*, **61**, 1–5 (1995).